



سازمان بنادر و دریانوردی به عنوان تنها مرجع حاکمیتی کشور در امور بندری، دریایی و کشتیرانی بازرگانی به منظور ایفای نقش مرجعیت دانشی خود و در راستای تحقق راهبردهای کلان نقشه جامع علمی کشور مبنی بر "حمایت از توسعه شبکه‌های تحقیقاتی و تسهیل انتقال و انتشار دانش و سامان‌دهی علمی" از طریق "استانداردسازی و اصلاح فرایندهای تولید، ثبت، داوری و سنجش و ایجاد بانک‌های اطلاعاتی یکپارچه برای نشریات، اختراعات و اکتشافات پژوهشگران"، اقدام به ارایه این اثر در سایت SID می‌نماید.



3D Numerical Study of Hydrodynamic Forces on Surface-Piercing Inclined Marine Piles

Mostafa Amini Afshar¹, Mohammad javad Ketabdari², Sabagh Yazdi³

1- Hormozgan University, Department of Civil Engineering

2- Amirkabir University of Technology (AUT), Faculty of Marine Technology

3-Khaje Nasir University, Department of Civil Engineering

Abstract

Inclined pile is a structural element which is widely used in variety of structures to confront the lateral forces in marine environment. Although study of wave forces on piles dates back to few decades ago, however many of these studies mainly focused on wave interaction with vertical piles. These results then roughly extend for inclined piles. This study focus on numerical estimation of the hydrodynamic wave forces on a Surface-Piercing Inclined Marine Pile to determine the hydrodynamic coefficients.

A set of tests performed on cylinders with different inclined angles in a numerical wave tank with a piston-type wave maker using Flow 3D. History of applied forces resulting from the model run and also Morison equation are used to extract hydrodynamic drag and inertia coefficients. The results showed that these coefficients are very sensitive to wave characteristics and pile inclined angles so that the tables in classical offshore texts mostly overestimate or underestimate these important factors.

Keywords: Inclined Marine Pile, 3D Analysis, Numerical simulation

1 Introduction

The landmark in the study of wave forces on piling dates at about 1950, (Morison et. Al, 1950), a research in which Morison found a particular relationship between the force and kinematics of the wave. One of the important assumptions in his work was that the characteristics of wave such as velocity and acceleration had not been influenced by the presence of the body in the medium. It should be noted that wave force due to diffraction can not be estimated using the Morison equation. Of the pioneering study of diffraction is that of Havelock (1940) in which he developed a linearized diffraction theory for small-amplitude water waves in deep oceans. Nonlinear simulation of wave-structure interaction problems in three dimensions was first presented by Issacson (1977) in a work where the interaction between waves and offshore structures was studied. Estimation of wave load on spar platforms was done numerically via a particular method that is called, VOF (volume of fluid) by Kleefsman and Veldman (unknown). They used this method to simulate the free surface displacement of the water. Sunder ,et al (1998) conducted an extensive experimental study of forces due to regular waves on inclined cylinders in which they derived coefficient of drag and inertia for inclined cylinders of various inclinations. He examined the relationships between hydrodynamic coefficients, inertia and drag coefficient, and the dimensionless Keulegan-Carpenter parameter, and finally found that hydrodynamic coefficients change dramatically for Keulegan-Carpenter numbers up to 4. Another experimental study for inclined cylinders that influence of various inclinations on the wave force is demonstrated, is that of Anandkumar et.al

¹ M.Sc in Marine structures

² Assistant Professor

³ Assistant Professor

(1994), in which by conducting a wave flume test they measured dynamic pressures around cylinder and finally obtained the resulting net forces. Effects of random seas also studied by Sunder et al (1999), an experimental study in which dynamic pressures on inclined cylinders have been measured.

2 Governing Equations

In this study applying the finite difference method, continuity and Momentum equations have been solved. The differential equations can be expressed in term of Cartesian coordinate, X, Y, Z. All equations are formulated with area and volume porosity functions. This formulation called *FAVOR* (Fractional Area/Volume Obstacle Representation method) and is used to model complex geometric regions. In this method obstacles can be defined by zero volume porosity regions. Generally in this method area and volume fractions are time independent. However these quantities may vary with time when moving obstacles are being modeled. The continuity and also Navier-Stokes equations underlie the basis of numerically simulation of wave tank in this study as follows:

$$V_F \frac{\partial \rho}{\partial t} + \frac{\partial}{\partial x} (\rho u A_x) + \frac{\partial}{\partial y} (\rho v A_y) + \frac{\partial}{\partial z} (\rho w A_z) = 0 \quad (1)$$

$$\begin{aligned} \frac{\partial u}{\partial t} + \frac{l}{V_f} \left\{ u A_x \frac{\partial u}{\partial x} + v A_y \frac{\partial u}{\partial y} + w A_z \frac{\partial u}{\partial z} \right\} &= -\frac{l}{\rho} \frac{\partial p}{\partial x} + G_x + f_x \\ \frac{\partial v}{\partial t} + \frac{l}{V_f} \left\{ u A_x \frac{\partial v}{\partial x} + v A_y \frac{\partial v}{\partial y} + w A_z \frac{\partial v}{\partial z} \right\} &= -\frac{l}{\rho} \frac{\partial p}{\partial y} + G_y + f_y \\ \frac{\partial w}{\partial t} + \frac{l}{V_f} \left\{ u A_x \frac{\partial w}{\partial x} + v A_y \frac{\partial w}{\partial y} + w A_z \frac{\partial w}{\partial z} \right\} &= -\frac{l}{\rho} \frac{\partial p}{\partial z} + G_z + f_z \end{aligned} \quad (2)$$

In these equations G_x, G_y, G_z are body accelerations, and f_x, f_y, f_z are viscous accelerations that for a variable dynamic viscosity μ are as follows:

$$\begin{aligned} \rho V_f f_x &= -\left\{ \frac{\partial}{\partial x} (A_x \tau_{xx}) + \frac{\partial}{\partial y} (A_y \tau_{xy}) + \frac{\partial}{\partial z} (A_z \tau_{xz}) \right\} \\ \rho V_f f_y &= -\left\{ \frac{\partial}{\partial x} (A_x \tau_{xy}) + \frac{\partial}{\partial y} (A_y \tau_{yy}) + \frac{\partial}{\partial z} (A_z \tau_{yz}) \right\} \\ \rho V_f f_z &= -\left\{ \frac{\partial}{\partial x} (A_x \tau_{xz}) + \frac{\partial}{\partial y} (A_y \tau_{yz}) + \frac{\partial}{\partial z} (A_z \tau_{zz}) \right\} \end{aligned}$$

Fluid configuration is defined in terms of a volume of fluid (VOF) function, $F(x, y, z, t)$. This function represents the volume of fluid per unit volume and satisfies the following equation:

$$\frac{\partial F}{\partial t} + \frac{l}{V_F} \left[\frac{\partial}{\partial x} (F A_x u) + \frac{\partial}{\partial y} (F A_y v) + \frac{\partial}{\partial z} (F A_z w) \right] = 0 \quad (3)$$

where A_x, A_y, A_z denotes fractional areas at the centers of cell faces normal to the x, y and z direction respectively. The basic procedure for advancing a solution through one increment in time, δ_i , consists of three steps:

Explicit approximations of the momentum equations, Eq. 2, are used to compute the first guess for new time-level velocities using the initial conditions or previous time-level values for all advective, pressure, and other accelerations.

To satisfy the continuity equation (Eq. 1) when the implicit option is used, the pressures are iteratively adjusted in each cell and the velocity changes induced by each pressure change are added to the velocities computed in step 1. Iteration is needed because the change in pressure needed in one cell will upset the balance in the six adjacent cells. In explicit calculations, iteration may still be performed within each cell to satisfy the equation-of-state for compressible problems.

Finally, when there is a free surface or fluid interface, it must be updated using Eq. 3 to give the new fluid configuration. Repetition of these steps will advance a solution through any desired time interval. At each step, of course, suitable boundary conditions must be imposed at all mesh, obstacle, and free-boundary surfaces.

3 Wave tank simulation

One of important aspects in simulating a wake tank is to specify its boundaries. The boundary conditions considered in this study is as follows:

3.1 K.F.S.B.C: Kinematic Free Surface Boundary Condition: this boundary condition relates the free surface velocity to its elevation. Linearized K. F. S. B. C for a wave type flow based on potential theory is as: $-\frac{\partial \phi}{\partial z} = \frac{\partial \eta}{\partial t}$ On $z = 0$

The numerical method that is used in this study deals with kinematic free surface boundary condition by the velocities that are set on every cell boundary between a surface cell and an empty cell.

3.2 D.F.S.B.C: Dynamic Free Surface Boundary Condition. Lineaeized dynamic free surface boundary condition for wave type flow, based on potential theory is as: $\eta = \frac{1}{g} \frac{\partial \phi}{\partial t}$

on $z = 0$. As we mentioned earlier, the numerical method is capable of modeling the free surface via the volume of fluid function (VOF) approach. The function represents fluid and void regions by 1 and 0 respectively. Dynamic free surface boundary condition is applied by assigning a uniform pressure to void region ($F=0$).

3.3 B.B.C: Bottom Boundary Condition. That specifies zero vertical velocity on the impervious bed, that based on the potential theory is as: $-\frac{\partial \phi}{\partial z} = 0$ At $z = -h$, in which h is water depth.

3.4 No-Flow condition on cylinder surface. For an impermeable cylinder is as: $-\frac{\partial \phi}{\partial n} = 0$ on cylinder surface. In which n is the vector normal to the surface. B.B.C and also no-flow condition on cylinder surface is applied to the wave tank by setting the normal velocity to zero. This is done by blocking the surfaces of bed and cylinder that otherwise are open to flow.

3.5 R.B.C. Radiation Boundary Condition.

For the practical reasons, both experimental and numerical wave tanks have to be of limited extent and inevitably we must truncate some boundaries of the wave tanks and as a result of this fact, waves have to propagate in a limited region.

Something of vital importance here is to prevent the outgoing waves, which are passing these truncated boundaries, from reflecting back into the wave tank. This is exactly the case in actual situation in which the waves reflecting away from the body never back towards it. In experimental wave tanks the problem overcome by using wave dissipaters, in numerical wave tanks, this is done via applying *Radiation Boundary Condition*. Based on the potential theory this condition is as: $\frac{\partial \phi}{\partial n} = \frac{1}{C} \frac{\partial \phi}{\partial t} = 0$

Where C wave celerity and n is the vector normal to the boundary. The present numerical method applies this boundary condition as: $\frac{\partial Q}{\partial t} + C \frac{\partial Q}{\partial x} = 0$ In which Q is any flow quantity.

3.6 Wave Boundary Condition.

Generally one side of wave tanks devoted to wave creation. In experimental studies this is done by wave makers. Based on the type of the wave that is wanted, there is variety of wave makers. In theoretical studies we can apply this boundary condition by specifying a particular velocity to one side of the wave tank. We use here of a piston type wave maker by applying the following displacement and velocity specifications:

$$x = \frac{S}{2} \sin \omega t, \quad u(0, z, t) = \frac{S}{2} \omega \cos \omega t$$

In which S is stroke of the wave maker

4 Specifications of the tests.

A set of 24 tests 4 carried out, in which angle of inclination of the cylinder varies up to 45 degree. For each angle the tests is repeated for four different KC , that are 4.3, 2, 0.87 and 0.5. Following specifications considered here to conduct the tests:

Wave tank: Height: 100 cm, Length: 270 cm for cylinders with $0^\circ, 15^\circ, 20^\circ, 30^\circ$ inclination, and 320 cm for 40° and 45° inclination, Width: 100 cm, Water depth: 30 cm
Side view and plan view of the wave tank that used for $\theta = 45^\circ$ is shown in fig. 1. Wave maker located at $z = 0.5$ and has the freedom to move between $-20 \leq z \leq 20$. At the distances more than three times of the water depth from the wave maker, standing waves decayed virtually (Dean and Dalrymple, 1992)

Cylinder: Diameter: 30 cm

Position: ($\theta = 0^\circ$ $z = 145$ cm), ($\theta = 15^\circ$ $z = 130$ cm), ($\theta = 20^\circ$ $z = 150$ cm), ($\theta = 30^\circ$ $z = 150$ cm), ($\theta = 40^\circ$ $z = 130$ cm), ($\theta = 45^\circ$ $z = 130$ cm)

Wave: Period: 1 sec for all tests.

Piston stroke: Varies for each KC as: ($KC = 4.3$ $S = 17.5$ cm), ($KC = 2$ $S = 10$ cm), ($KC = .87$ $S = 5$ cm), ($KC = .5$ $S = 3$ cm)

Finish time: The model is run up to 10 wave periods that is 10 sec.

5. Conducting the tests

24 distinct tests was carried out each of which having a particular N_K and θ . In these tests the focus was on forces applied to the cylinders in the z direction. Each run

terminated with a history plot of the net pressure force in z direction. Fig. 2 shows these results for different KC and θ .

6. Extracting Hydrodynamic Coefficients.

According to the Morison equation; maximum drag and inertia forces correspond to the maximum velocity and acceleration respectively. On the other hand velocity and acceleration in wave kinematics are 90 degrees out of phase. This means that at the time of maximum velocity, acceleration becomes zero and vice versa. We make use of this fact and for calculating of inertia and drag coefficients, equate the forces resulting from the model, at the time of maximum velocity and acceleration, with those of estimated by the Morison equation.

7. Results and Conclusions

According to Sundar (1997), more or less drag coefficients become independent of inclination of the cylinder at KC greater than 4. This was the base to pay particular attention on KC of 0.5, 0.87, 2 and 4.3. The results of the study show that both of drag and inertia coefficients decreases as KC increases. This is consistent with the trend line obtained by Sundar (1997). Furthermore it is observed from the figures that for $KC < 1$, inertia coefficients have a direct relationship with θ . However for $KC > 1$ the relation reverses and consequently C_M decreases as θ increases. In fig. 3 the drag coefficient has a minimum value at about $\theta = 25^\circ$. Although the values of C_D for $KC = 0.5$ seem to be strange but this interesting trend observed generally for all KC 's in this study.

Our attempt here in this study was really a minor step towards finding out hydrodynamic coefficients that may be utilized for estimation of wave forces on inclined cylinders via the Morison equation. Throughout the study we assumed a linear wave that impinges on the cylinder. In this regard to ascertain of actual situations in ocean, random seas and irregular waves, the study needs to be continued by applying non linear waves to cylinder. Moreover the cylinder and the bed was impervious in our study, something that may not be the case in actual situations, thus another studies could be carried out by pervious bed and cylinders.

9. Reference

1. Anandkumar, G., Sundar, V., Graw, K.U. and Kaldenhoff, H., (1995): "Pressure and Forces on Inclined Cylinders due to Regular Waves", Journal of Ocean Engineering Vol.22, pp 747-759
2. Havelock, T.H., (1940): "The Pressure of Water Waves on Fixed Obstacles", Pro. Roy. Soc.Lond.
3. Issacson, M. St. Q. (1977): "Non Linear Wave Forces on Large Offshore Structures", Journal of Waterways port Coastal and Ocean Engineering.
4. Morison, J.R., O'Brien, M.P., Johnson, J.W., and Schaaf, S.A. (1950): "The forces Exerted by Surface Waves on Piles", Petroleum Transactions.
5. Rahman, M., Satish, M.G. and Xiang, Y., (1992): "Wave Diffraction due to Large Offshore Structures", A Boundary Element Analysis. Journal of Ocean Engineering Vol.19, pp 271-287
6. Dean, R., G. and Dalrymple, R. A., (1992): "Water Wave Mechanics for Engineering and Scientists", World Scientific, London, UK.

7. Sundar, V., Koola, P., M., Schlenkhoff, A.U. (1999): "Dynamic Pressures on Inclined Cylinders due to Freak Waves", Journal of Ocean Engineering Vol.26, pp 841-863

8. Sundar, V., Vengatesan, V., Anandkumar, G., and Schlenkhoff, A. (1998): "Hydrodynamic Coefficients for Inclined Cylinders", Journal of Ocean Engineering Vol.25, pp 277-294

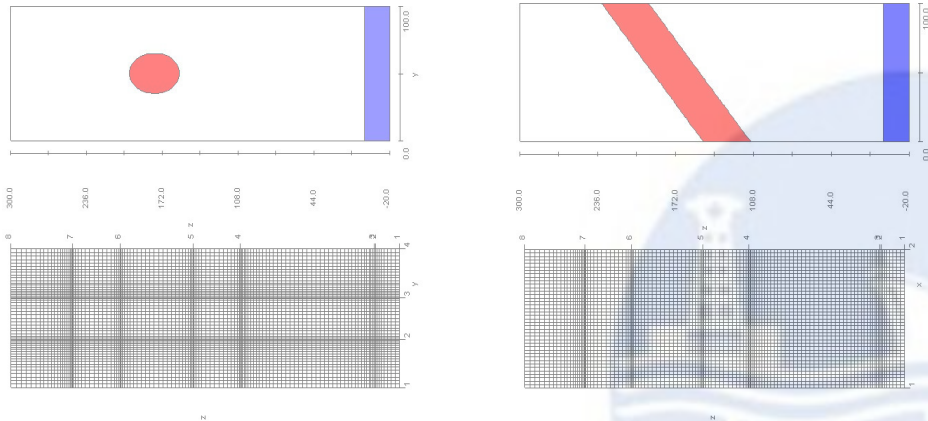


Figure 1 Side and plan view of numerical wave flume and inclined cylinder

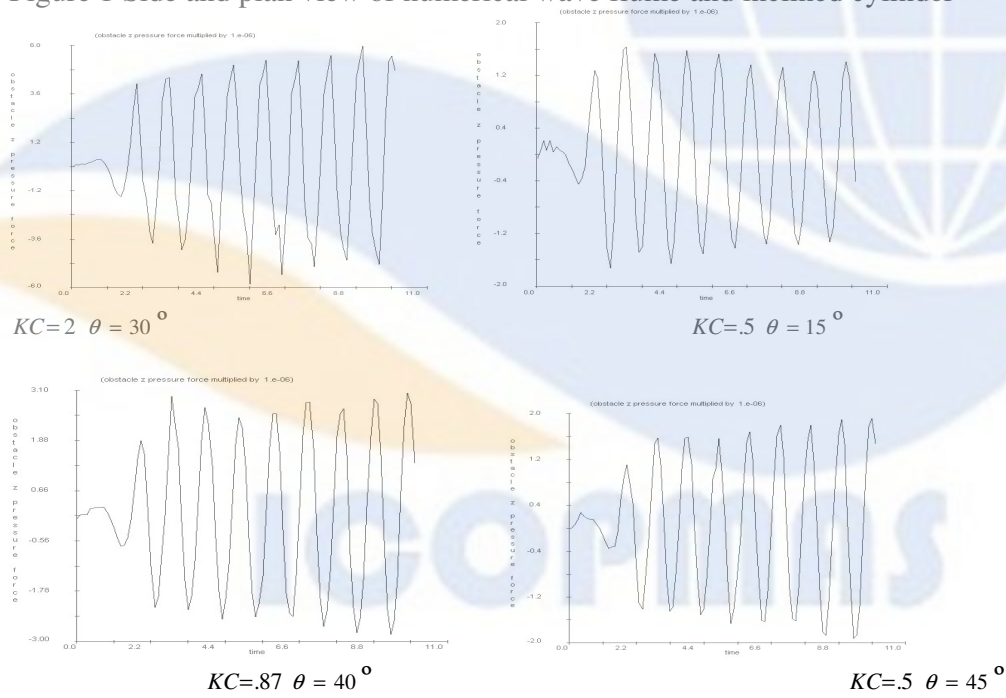


Figure 2 pressure force time history for different KC and θ .

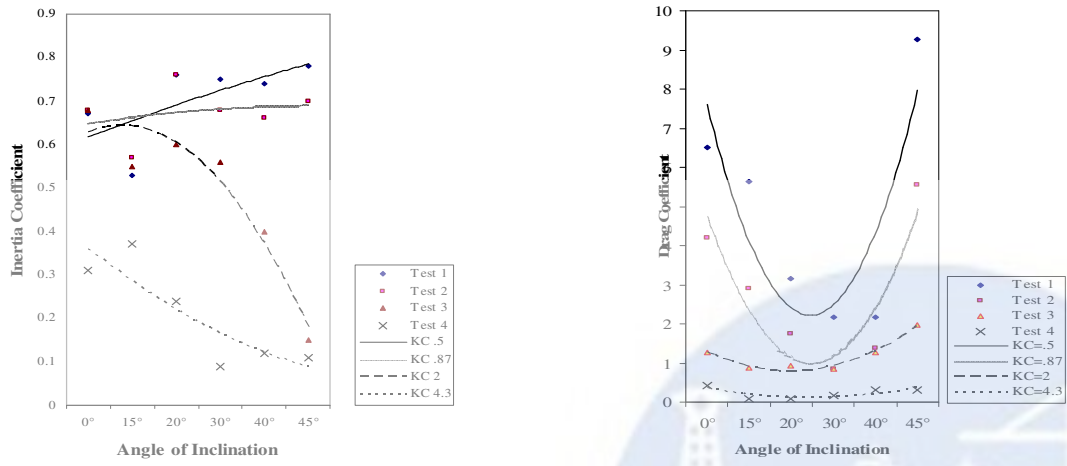


Figure 3 Inertia and drag coefficients due to waves versus angle of inclination

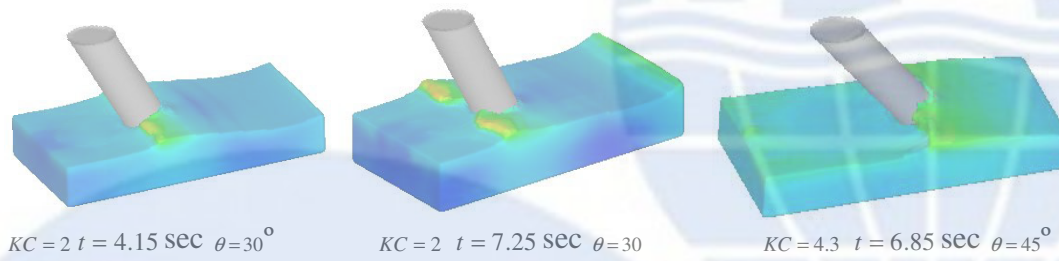


Figure 4 Instantaneous surface elevations of the flow around inclined cylinder